Human-Like Artificial Skin Sensor for Physical Human-Robot Interaction

Marc Teyssier[1,2], Brice Parilusyan[2], Anne Roudaut[3] and Jürgen Steimle[1]

***Abstract*— Physical Human-Robot-Interaction (pHRI) is beneficial for communication in social interaction or to perform collaborative tasks but is also crucial for safety. While robotic devices embed sensors for this sole purpose, their design often is the results of a trade-off between technical capabilities and rarely considers human factors. We propose a novel approach to design and fabricate compliant Human-like artificial skin sensors for robots, with similar mechanical properties as human skin and capable of precisely detecting touch. Our artificial skin relies on the use of different silicone elastomers to replicate the human skin layers and comprises an embedded electrode matrix to perform mutual capacitance sensing. We present the sensor and describe its fabrication process which is scalable, low-cost and ensures flexibility, compliance and robustness. We introduce *Muca*, an open-source sensing development board and then evaluate the performance of the sensor.**

I. Introduction

Robots are increasingly present in the physical environment. Direct Human-Robot-Interaction is therefore a key feature to ensure safety and adapt robotic behaviour to a user's interaction. Detecting direct touch interactions and contacts is an ongoing challenge in robotics, particularly in collaborative and social robotics, where robots must be able to sense the interactions and predict the user's intent. During human-human social interactions, touch is performed and interpreted through the skin. This sensing organ is ubiquitous, covers our whole body and we know how it behaves when we touch it. While artificial skin sensors have been developed to widen the robots' sensing capabilities, the current solutions do not yet combine robust sensing with familiar human-like look and feel. We argue that replicating the mechanical properties of human skin to design an artificial robotic skin could promote intuitive interactions with robots and is a new step towards user-friendly humanoid robots and physical Human-Robot Interaction (pHRI) [1], [2], [3].

Different approaches to design and fabricate artificial skin have been proposed [4], [2], [5], [6]. Force-sensing resistors (FSR) were traditionally used to sense touch because of their accessibility [7] and their relatively low cost. They motivated the development of resistive [8] or piezo-resistive [9] robotic skins and were implemented in robotic systems [10], [11]. These sensors can effectively sense human touch but tend to be hard to implement. They often consist of a sandwich of conductive rubber or textile [12], [13], [14], [15], [16], resulting in a complex fabrication process and wiring. Capacitive sensing is nowadays the most commonly used technique [6]. It presents a lower hysteresis, but its fabrication method is as complex as those of resistive or piezo-electric robotic skin.

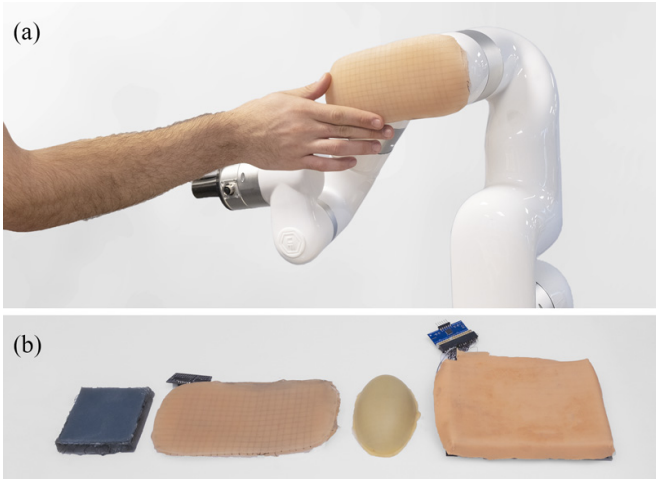

Fig. 1: a) Human-Like Artificial Skin Sensor on a *xArm 6*'s joint. b) The fabrication method allows to create flexible sensors with different shapes and mechanical properties.

Covering a large surface of a robot generally makes use of distributed arrays of discrete sensors, also referred as *skin patches* [17] or *taxels*[18]. Although this technique provides a relatively high density of sensors, they are often attached to underlying PCBs (see [12], [19]) which do not strictly conform to the robot's surface. Moreover, the multiplication of electronic components increases the cost and requires a complex network architecture [20], [21]. The design of a skin sensor is often a trade-off between sensor resolution, accuracy or robustness. Few artificial skin sensors consider reproducing the comfort and tactile properties of human skin. Efforts are made to hide the sensor behind the robot skin and render a comfortable touch. To replicate the softness of the skin, some sensors embed a soft cushion layer [22], [11] or cover the sensing elements with textile, for instance on the iCub robotic platform [18]. Other sensors are covered with silicone-based materials to give a more "pleasant" and human-like feel [23], [24], [25]. Overall, the human-like and comfort aspect is seen as an extra layer covering the sensing technology. We argue that comfort aspects should be given equal priorities than technical characteristics during the design process. Not only would it provide better sensor integration over a robotic device but also offer opportunities in terms of improved robustness and performance.

[1]Saarland University, Saarland Informatics Campus, Germany. Contact: contact@marcteyssier.com
[2]Pôle Universitaire Léonard de Vinci, Research Center, France
[3]Bristol Interaction Group, University of Bristol, UK
This project received funding from the European Research Council (ERC StG Interactive Skin 714797).

Anthropomorphism is commonly used to design humanoid robots, yet the design of skin sensors rarely follow these principles. We follow the tradition of human-friendly artificial skin [26], [27] and adopt specific requirements for the design of our sensor:

1) The tactile acuity (or *resolution*) of artificial skin should be high and allow to detect complex tactile information, such as single touch or multi-touch finger pressure, location or shape.
2) The artificial skin should be soft, comfortable to touch and have haptic properties similar to human skin.
3) The geometry and materials of artificial skin should be compliant to fit the robot's curved surfaces and cover large surfaces.
4) The artificial skin should be low-cost and easy to fabricate in order to foster replication and widen its use within the robotic community.

Based on these requirements, we propose a novel human-like artificial robotic skin sensor that reproduces the kinesthetic properties of the skin while providing robust touch sensing capabilities. The design of this sensor draws inspiration from the three main layers the human skin is composed of: *epidermis*, *hypodermis* and *dermis*. We use silicone elastomers with different properties to reproduce the *epidermis* and *hypodermis* layers. These layers provide realistic touch feedback, softness and flexibility and make the sensor both adaptive to the robot's shape and comfortable for the user to touch (Fig. 1b). To sense touch, we rely on projected mutual capacitance, which detects human touch by measuring the contact force and contact area with a high acuity.

This work aims at improving pHRI by proposing an artificial skin that is precise, robust, low cost, deformable, familiar and intuitive to use and that can be easily replicated by Robotics practitioners. We build upon a previously published prototype [28] in Human-Computer Interaction. In this paper, we improve the previous iteration and describe in detail the sensor working principle and present its fabrication method, open-source electronics and signal processing pipeline. We then evaluate the sensor response to touch, force, its spatial resolution and the effect of curvature. Finally we present an implementation for a robotic arm (Fig. 1a).

II. Methods and Apparatus

A. Design Considerations

We use the human skin layers as a guideline to reproduce their sensing capabilities and mechanical properties in the presented sensor. Three main layers compose the human skin and influence its mechanical response to stretch, strain and pressure as well as its tactile perception abilities. First, the *epidermis* is the external and visible part of the skin. It has a variable thickness between 0.3mm and 1mm [29] and a typical surface texture. This layer is solid and acts as a barrier to the external world. The *hypodermis* is the bottom-most and thickest part of the skin. It is considered as viscoelastic [30], measures around 10mm and is primarily

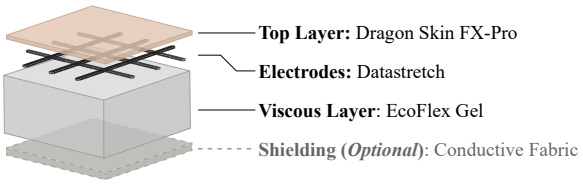

Fig. 2: Layered structure of the sensor. The sensing electrodes are situated in-between two layers of silicone with different mechanical properties.

composed of body fat. It provides mechanical support to the other layers and acts as a natural cushion when we compress the skin. Finally, the *dermis* layer is located in-between these two layers. With a thickness that varies between 0.9mm and 2.5mm, this layer can resist to high tensile strength and comprises our touch sensing nerves [31], [32], which respond to tactile and kinesthetic stimuli. The density of the tactile receptors depends on the location on the body. Overall, the skin spatial acuity is in the order of 8mm, with a variation from 2.3 mm inside the palm, 7mm on the forearm and up to 15mm on the thigh [33], [34], [35].
These design considerations inform the inner layers of the sensor, impact the choice of material and define the requirements for the sensing method.

B. Sensing Principle

The sensing principle is based on projected mutual capacitance. This technology is the industry standard for multi-touch sensors and identifies touch by measuring the local change in capacitance on a grid array of conductive traces (or electrodes) in X and Y directions. At each electrode cross-section, a capacitor is formed, hence creating $X \times Y$ capacitors on the surface. When a human finger gets close, capacitance coupling between the two electrodes is reduced as the electric field between them is disturbed by the finger (Figure 3-a). When the two electrodes get closer, the mutual-capacitance coupling increases. There are two types of electrodes, one in each direction: the emitting electrodes and sensing electrodes - conventionally called *transmit* electrodes (*Tx*) and *receive* electrodes (*Rx*). To measure a capacitance, we sequentially apply an excitation signal to each *Tx* electrode while *Rx* measures the received signal. A user's touch decreases the mutual capacitance (C_M) between

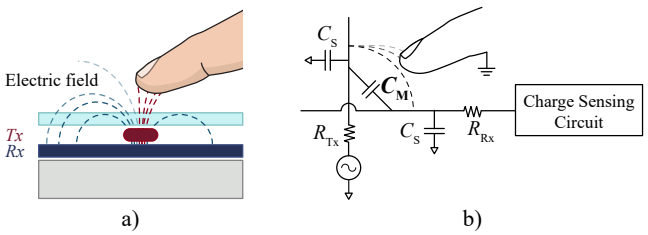

Fig. 3: The sensing principle is based on projected mutual capacitance. a) A finger approaching a cross-section of Rx and Tx electrodes disturbs the nearby electric field and decreases the capacitance (C_M) between the electrodes. b) Equivalent circuit diagram.

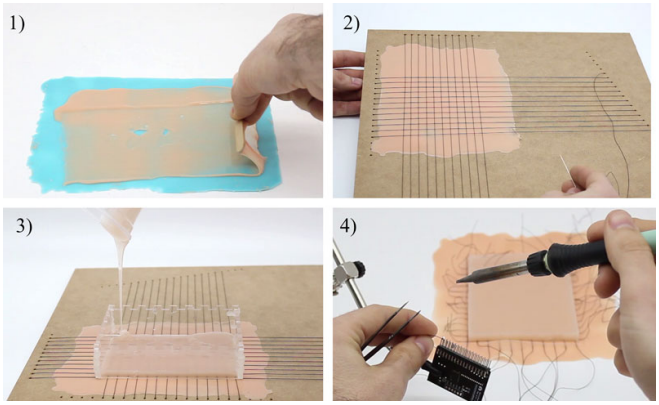

Fig. 4: The fabrication process of the sensor is easy and requires only little fabrication skills. 1) Prepare the external layer. 2) Position the electrodes in a grid pattern. 3) Add a layer of viscous silicone. 4) Solder the electrodes to the electronic board.

the electrodes by 0.1pF up to 2pF (Figure 3-b). Different electrode patterns impact the reading precision [36]. One advantage of mutual capacitance over self-capacitance or resistive arrays is that it can capture true multi-touch input, reduce ghost points [37] and detect a finger hovering prior to touch. Our sensor uses a rectangular electrode pattern that consists of a simple overlapping of straight lines. This pattern is slightly less efficient than the common diamond pattern, nonetheless it is much easier to implement and fabricate, as demonstrated in the following sections. The spacing and thickness of the electrodes affect the overall resolution and the absolute capacitance measurements at a given point.

C. Sensor Material And Fabrication

Skin Material Choice. To fabricate the sensor, we use various platinum cured silicone products from Smooth-On Inc. The silicone is used in soft robotics [18], [38] because of its variable strain resistance and viscoelasticity, which makes it the ideal material to reproduce the different skin layers.To create the top external layer (*epidermis*), we use Dragon Skin Fx-Pro (Smooth-On Inc). This silicone has a shore hardness of 2A and is often used to create flesh-like prosthetics because its surface texture is close to human skin [39], [40], [41] and it can also be pigmented.The *hypodermis* is made with EcoFlex Gel (Smooth-On Inc) which is an extremely soft (negative shore hardness of 000-35) and flexible silicone with human fat-like mechanical properties [42], [43].

Electrode Material. Inspired from the sensitive middle layer of human skin, the *dermis*, the middle layer of our sandwich comprises the sensing electrodes. These are the critical elements to perform an efficient mutual capacitance measurement. While conductive elastomers are often used to create robotic skin [44], their electrical resistance is often too high to detect changes in the order of *pF*. Moreover, it is difficult to manually coat and successively overlap patterned layers. For this reason, we decided to use an off-the-shelf conductive yarn (*Datastretch* by *TibTech*). The yarn is made of copper, is 0.2mm thick, with a conductivity of 4.2Ω/m and is stretchable up to 30%. Its small thickness and high stretchability provide a thin sensing layer while maintaining compliance with silicone properties. The yarn is also electrically insulated and hence does not require a complementary dielectric layer between the electrodes.

Fabrication. The sensor fabrication requires little skills in digital fabrication and follows a four-step process (Figure 4).

1) Create a thin (about 1mm) layer of *Dragon Skin FX-Pro* that acts as *epidermis* and insulates the sensing electrodes from direct touch. This layer can optionally be casted over a textured skin mold [23].
2) Position the electrodes on top of this layer, that acts as *dermis*. A guide is used to create a grid layout and to ensure an even spacing between between the electrodes.
3) Add a thick layer of *Ecoflex Gel* (about 10mm) on top of the electrodes, that acts as *hypodermis*. This allows malleability, bonds the electrodes between the two silicones layers and ensures robustness when the sensor is strained.
4) Solder the electrodes to the dedicated sensing board.

This fabrication process has the advantage to encapsulate the sensing electrodes between different skin layers, ensuring robustness and durability. The overall interface can be cut to any shape (see Fig. 1b), is soft to touch and can absorb collision energy. Unlike previous works that rely on underlying rigid or semi-flexible PCBs [12], [45], [46], [21], the artificial skin is completely flexible, resistant to shear and stretch and can be conformed to 3D curved surfaces of the robot. The electrodes are connected to the sensing board, which can lie on the side of the sensing area. An additional layer of shielding [12] can be positioned under the *hypodermis* layer to decrease background noise.

D. Hardware Sensing

For the sensing, we developed *Muca*[1] (Fig. 5), an open-source mutual capacitance sensing development board. The board features a single-chip capacitive touch panel controller IC *FT5316DME* MCU by FocalTech. The controller board allows to easily connect 21 *transmit* electrodes and 12 *receive* electrodes by exposing 33 pins. This design enables to solder driving electrodes (transmit/receive) of up to 15kΩ, and is well-suited to sense mutual capacitance from $1pF$ to $4pF$. The chip uses two wires for serial communication via I^2C interface to a host processor, provides an optional interrupt signal and needs two wires for the 3.3V energy supply. The board is low-power and uses about $0.05mAh$ per scan.

The board offers two control modes: *Touch Point* and *Raw Scanning*. In *Touch Point* mode, the controller uses an on-chip algorithm to calculate and detect up to 5 finger contacts. The controller shares the XY coordinates as well as the contact area at a 60Hz rate. This mode is suitable for fingertip touch only, but not for advanced touch detection. The *Raw scanning* mode reads raw mutual-capacitance values of all electrode intersections, with a 16 bit resolution. Built-in hardware gain provides additional level of control

[1]Development board available at https://muca.cc

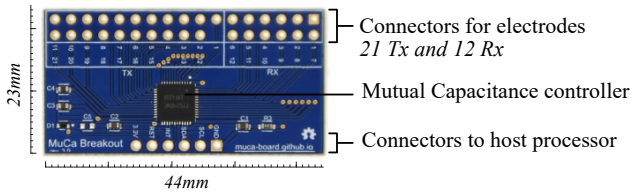

Fig. 5: Open-source *Mu*tual *Ca*pacitance development board (*Muca*), exposing 33 pins to connect custom electrodes.

over the measurement range and noise. The entire sensor surface is scanned at a rate of 40Hz, and the resulting raw capacitance data can be processed using standard computer vision algorithms.

E. Signal Processing and Touch Detection

The signal processing pipeline is divided into two main steps: first, the digital hardware calibration, and second, computer vision. An initial calibration is needed to remove the variance of the capacitance baseline (about 200 units). This is due to the manual fabrication of the sensor as well as the quality of the soldering to the board. We create a baseline calibration matrix, filled with the average of 16 consecutive readings for each mutual capacitance value. For every incoming mutual capacitance measurement, we subtract the baseline and apply a threshold to remove the 95% percentile, considered as background noise.

Computer vision algorithms are used to analyze the signal and detect touch location. We normalize the array of mutual-capacitance values after the transformation by the calibration and store them in a 2D image file of 12x21 pixels resolution (Fig. 6b. This image is then up-scaled 30 times using the Lanczos-4 algorithm, which increases its resolution while supporting an accurate spacial interpolation (Fig. 6c).

Two main types of intentional gestures are commonly performed on a robot: simple touch with the tip of the finger and more complex touch (Fig. 6a). To track single finger or multiple finger touch, we first identify distinct elements in the image. We convert the grayscale image into a binary image with a 55% threshold and apply *contour* and *blob* detection (Fig. 6d). We calculate the relative area of each segmented

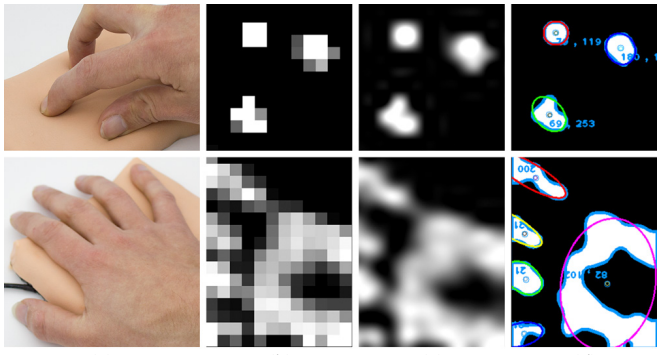

(a) (b) (c) (d)

Fig. 6: Signal processing pipeline. (a) Examples with finger touches and complex gesture. (b) Raw measurements from the sensor after calibration. (c) Up-scaled data using CV. (d) Blob detection to extract touch location and area.

element and compute their nearest fitting ellipsoid. The center of the ellipsoid defines the touch point location and the area can provide information about the touch pressure. This image processing lasts for about 4ms. To track touch movement over time, the contour points are stored in a K_d tree and every new frame we retrieve the closest blob position in O(log$n$). Advanced gestures differ from simple touch contact by their larger areas of contact and their specific dynamic. Standard approaches for detecting advanced touch gestures can be applied on the capacitive images [47], [48], using image segmentation or by discriminating the shape of the blobs, their orientation and eccentricity as well as their displacement over time.

III. Sensor Characterization

In this section, we present the characterization of the skin sensor. We characterize the properties of a single sensing capacitor and the touch processing algorithm on the entire interface. The evaluation was conducted using a skin sensor (Fig. 1, bottom-right) with a $96mm$ width, $138mm$ length, a $15mm$ height (depth) and an electrode spacing of $8mm$. The sensor was mounted on a specialized test bench. The test bench consisted of a hemispherical effector probe with a $15mm$ diameter, mounted on a rig controlled in X, Y and Z positions. The Z-axis origin was set at the exact contact location between the effector's head and the skin surface. The effector was then displaced in the Z axis to apply normal perpendicular load forces.

A. Mechanical Response

We first conducted an initial mechanical characterization to better understand how the artificial skin mechanically responds to contact force. We measured the relation between the probe penetration in the material as well as the applied force. We moved the probe with $1mm$ increments, up to a $5N$ force. The results are presented in Fig. 7. We can see a logarithmic relationship between the distance and the applied force. The first $4mm$ show a higher stiffness and resistance than the last one. This is in-line with the biomechanical properties of human skin [49] and suggests that the mechanical behavior of the silicone layers is close to human skin. This result can be explained by the stress distribution inside the *hypodermis* layer, but requires more experimental results to be confirmed. The physical compression might also affect the global thickness of the dielectric between the electrodes, which can provide a better response to contact force.

B. Signal-to-Noise Ratio

As a first sensor characterization, we calculated the SNR (Signal-to-Noise Ratio) of a cross-section of the uncalibrated sensor using the formula (1) (in decibels, dB). We measured the signal *with* and *without* contact force 20 times for each hardware gain (30 levels). μ_{nF} and σ_{nF} are the average and standard deviation values when there is no contact, and μ_F is the average value with contact force applied.

$$SNR_{dB} = 20log(\frac{|\mu_{nF} - \mu_F|}{\sigma_{nF}})dB \quad (1)$$

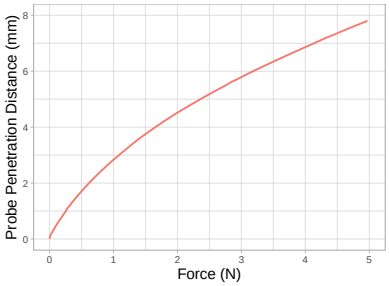

Fig. 7: The penetration distance over the applied force suggests a mechanical resistance in the first millimeters. This is consistent with the properties of human skin.

The results range from $60dB$ to $25dB$ and are presented in Figure 9a. A higher hardware gain reduces the SNR and affects the working range of the sensor (Fig. 9b). These results are above 15, the minimum required for robust touch sensing [50] and are in line with existing robotic skin sensors [51]. The noise and sensitivity does not significantly vary between different manufactured sensors and remain similar for all cross-sections of the same sensor.

C. Response to Force

We evaluated the sensor response to different levels of force. With the probe positioned above one electrode cross-section of electrodes, we moved up and down in increments of $0.1mm$, from $0N$ to $5N$ ($-8mm$ into the surface). After each step, we measured the applied force and the raw mutual capacitance value (Gain 8). This whole process lasted 2.2 seconds and the operation was repeated 50 times.

Figure 8 shows the response to force, hysteresis and repeatability properties of our sensor. The sensor response follows a logarithmic curve. This non-linear response can be explained in part by the mechanical response of the silicone. The sensor is responsive to low pressure, and has a good precision to detect forces above $0.5N$. Results show a low hysteresis: we measured a negligible difference of 2 measurement units between the press down and up. Figure 8 shows the measurement envelopes for each repetition. The sensor has repeatable results, with an average standard deviation of 4 units and average mean deviation of 11.

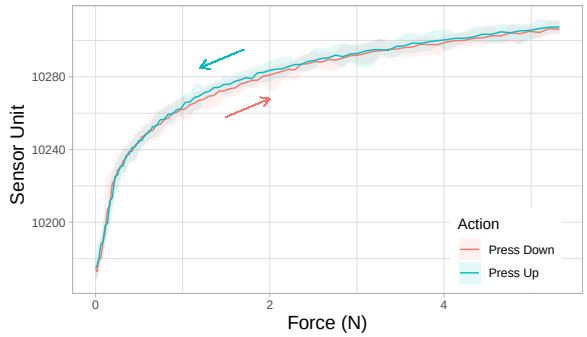

Fig. 8: Sensor response to normal force. The red and green lines represent the mutual capacitance values, read during the press down and press up, respectively.

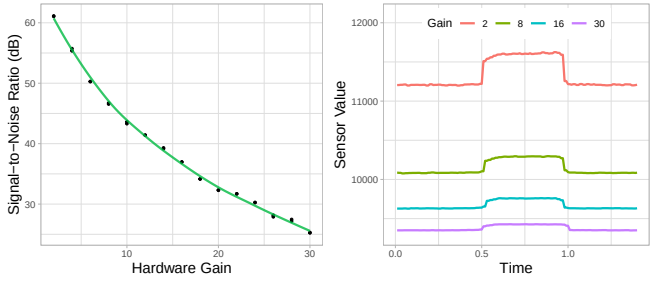

(a) (b)

Fig. 9: Effect of hardware gain on SNR. The same sensor can be used for sensitive or robust touch by fine tuning of the gain. a) SNR for different gain values. b) Example with four touch contacts (finger pressed down from 0.5s to 1s).

D. Spatial Acuity

To characterize the spatial acuity of the sensor, we defined a 6 x 5 matrix of points on the sensor, with each point separated in X and Y directions by 1 cm. While the spatial resolution at a hardware level is defined by the electrode spacing, $8mm$ in our case, our experiment uses the higher-resolution interpolated values generated by the signal processing described above. The test bench sequentially applies $5N$ of normal force to each point and we compute the center of the touch point (*blob*). This operation was repeated 15 times for each point. To measure the spatial acuity, we measured the relative distance between the software calculated center position and the real ground truth position, and computed its average.

The signal processing pipeline provides a $0.5mm$ spatial acuity (standard deviation = $0.2mm$). Eventual variations in the top layer surface thickness does not impact the precision of the sensor. This result is encouraging, as it is higher than the acuity of human skin (with its $8mm$ average) [33] and the resolution of most existing sensors (e.g [52], [14], [21]).

E. Curvature Effect

The sensor does not have an underling solid structure, hence it can be deformed and conformed to curved surfaces. We conducted measurements to analyse the effect of curvature on the sensing capabilities. As a baseline, we performed a measurement with the sensor placed on a flat surface. We then conducted another series of measurements with the sensor bent over a curved object, a cylinder with $5cm$ radius. Similar to the previous tests, the probe was positioned in contact with the surface and was moved in the Z-direction in increments of $0.1mm$ up to $5N$. This was repeated 50 times.

The results are presented in Figure 10a. There is a strong correlation between the two curves (*Pearson's r=0.996, p<0.0001*), which suggests curvature does not affect the sensor. However, we can see a different behaviour in the $0N - 1N$ range (Fig. 10b). This effect might be due to a response of silicone to bending, and should be further explored in future work.

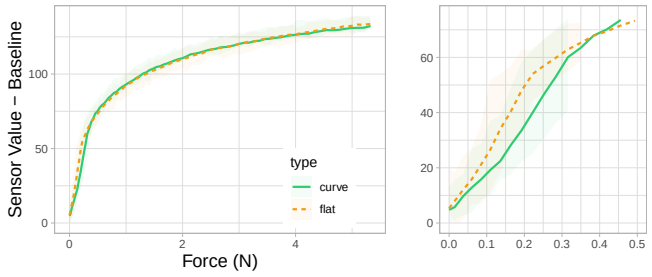

(a) (b)

Fig. 10: a) Calibrated sensor response to Z-axis force on a flat and curved surface. b) Zoom in the $0N$-$0.5N$ range. The curvature of the sensor can induce a small variation in the response to low pressure.

IV. System Integration

As an initial exploration, we attached a robotic skin to a *xArm 6* by *ufactory* as seen on Figure 1. The artificial skin is built to conform to the curved surface of the joint ($90mm$x$180mm$x$10mm$) and has an electrode spacing of $7mm$. The sensor is shaped by cutting the corners with scissors and attached to the robot. The *Muca* board is connected to an *Arduino Nano* and communicates with the computer vision software. We programmed the robot to react to touch contact, to ensure the user's safety: if a sudden collision is detected (*blob* with large size), the motion of the robot is stopped to prevent the user to be hurt.

Beyond safety, this sensor is ideal for social robotics and collaboration. It is known that social and affective touch plays a crucial role for communication [53], [3]. And within this context, the skin is a fundamental biological interface to sense the world and communicate with others [54].

Gesture recognition algorithms could also help understand the users' intended actions and behave accordingly to them. The sensor is detecting multi-touch contact points with a high tactile acuity, making it adapted to recognize expressive gestures such as tickling, stroking or pinching. Compared to other social-touch skin sensor[55], we achieve a high resolution while keeping a human-like look and feel. As application example, we built sensors with different shapes, curvatures, colors or thicknesses (Fig. 1 and Fig. 11), which can satisfy various social and cultural norms.

Fig. 11: The sensor can be shaped to conform to any robot. Here, a skin sensor is attached to a *Nao* social robot.

V. Conclusion and Future Work

A. Conclusion

We presented a human-like artificial skin sensor for physical Human-Robot Interaction. The interface is made of different layers of silicone and a grid of conductive yarn that is used to perform mutual capacitance sensing at a high resolution and high update rate. Collaboration and safety are critical challenges in Human-Robot Interactions, and can be enhanced through artificial skin. Our approach focuses on reproducing the mechanical and sensing properties of human skin. The proposed flexible sensor is simple in its design, easy to manufacture, mechanically robust, and conforms to curved surfaces. Our development board allows to measure touch with a high accuracy, high repeatability and low hysteresis. Results show that the sensor skin is able to sense a force up to $5N$ and to detect touch with an accuracy of $0.5mm$ at a 40Hz rate over the full surface. Furthermore, we demonstrated that the sensor can be used on a curved surface without impacting its reading performance, which ensures its ease of integration on a robotic arm to promote intuitive and safer physical interaction.

B. Future work

Our initial results for characterizing the sensor response to normal forces are promising. Future tests are planned to evaluate the sensor performances according to other forces, such as shear, stretch, or strong collisions. We plan to characterize the sensor's response to variable hypodermis thicknesses and evaluate the effect of electrode spacing over the spatial resolution. Moreover, the observed two-point discrimination threshold of the prototype is around 15mm and needs to be further investigated. The next step towards a full-body artificial skin for social robots requires to fully cover a humanoid robot with our artificial skin. Future work should focus on the scalability of the system. While another development board is currently being built to allow for more electrodes pin out and a more compact form factor, it is also worth exploring how several skins can be interconnected and how they can conform to a wide range of robotic link geometries and shape. Another area of research with this device is the detection of non-grounded objects. The sensor response depends on capacitance, and the initial calibration can be impacted by environmental changes (e.g. humidity). Future work will investigate real-time calibration and the integration of a shielding layer made of conductive textile.

ACKNOWLEDGMENT

This project received funding from the European Research Council (ERC StG Interactive Skin 714797) and the Engineering and Physical Sciences Research Council EPSRC EP/P004342/1. We would also like to thank E. Bouzbib for her constructive feedback.

References

[1] T. Minato, M. Shimada, S. Itakura, K. Lee, and H. Ishiguro, "Does gaze reveal the human likeness of an android?" in Proceedings. The 4th International Conference on Development and Learning, 2005. IEEE, 2005, pp. 106–111.

[2] D. Silvera-Tawil, D. Rye, and M. Velonaki, "Artificial skin and tactile sensing for socially interactive robots: A review," Robotics and Autonomous Systems, vol. 63, pp. 230–243, 2015.

[3] M. Teyssier, G. Bailly, C. Pelachaud, and E. Lecolinet, "Conveying emotions through device-initiated touch," IEEE Transactions on Affective Computing, 2020.

[4] M. H. Lee and H. R. Nicholls, "Review article tactile sensing for mechatronics—a state of the art survey," Mechatronics, vol. 9, no. 1, pp. 1–31, 1999.

[5] M. I. Tiwana, S. J. Redmond, and N. H. Lovell, "A review of tactile sensing technologies with applications in biomedical engineering," Sensors and Actuators A: physical, vol. 179, pp. 17–31, 2012.

[6] H. Akhtar, Q. Kemao, and R. Kakarala, "A review of sensing technologies for small and large-scale touch panels," in Fifth International Conference on Optical and Photonics Engineering, vol. 10449. International Society for Optics and Photonics, 2017, p. 1044918.

[7] S. Yeung, E. Petriu, W. McMath, and D. Petriu, "High sampling resolution tactile sensor for object recognition," IEEE Transactions on Instrumentation and Measurement, vol. 43, no. 2, pp. 277–282, 1994.

[8] J. Klimaszewski, D. Janczak, and P. Piorun, "Tactile robotic skin with pressure direction detection," Sensors, vol. 19, no. 21, p. 4697, 2019.

[9] G. Canavese, S. Stassi, C. Fallauto, S. Corbellini, V. Cauda, V. Camarchia, M. Pirola, and C. F. Pirri, "Piezoresistive flexible composite for robotic tactile applications," Sensors and Actuators A: Physical, vol. 208, pp. 1–9, 2014.

[10] T. Asfour, K. Regenstein, P. Azad, J. Schröder, and R. Dillmann, "Armar-iii: A humanoid platform for perception-action integration," in Proc., International Workshop on Human-Centered Robotic Systems (HCRS), Munich. Citeseer, 2006, pp. 51–56.

[11] T. Mukai, M. Onishi, T. Odashima, S. Hirano, and Z. Luo, "Development of the tactile sensor system of a human-interactive robot "riman"," IEEE Transactions on robotics, vol. 24, no. 2, pp. 505–512, 2008.

[12] J. Ulmen and M. Cutkosky, "A robust, low-cost and low-noise artificial skin for human-friendly robots," in 2010 IEEE International conference on robotics and automation. IEEE, 2010, pp. 4836–4841.

[13] C. Honnet, H. Perner-Wilson, M. Teyssier, B. Fruchard, J. Steimle, A. C. Baptista, and P. Strohmeier, "Polysense: Augmenting textiles with electrical functionality using in-situ polymerization," in Proceedings of the 2020 CHI Conference on Human Factors in Computing Systems, 2020, pp. 1–13.

[14] M. Strohmayr, H. Wörn, and G. Hirzinger, "The dlr artificial skin step i: Uniting sensitivity and collision tolerance," in 2013 IEEE International Conference on Robotics and Automation. IEEE, 2013, pp. 1012–1018.

[15] J. O'Neill, J. Lu, R. Dockter, and T. Kowalewski, "Stretchable, flexible, scalable smart skin sensors for robotic position and force estimation," Sensors, vol. 18, no. 4, p. 953, 2018.

[16] J. Park, Y. Lee, J. Hong, Y. Lee, M. Ha, Y. Jung, H. Lim, S. Y. Kim, and H. Ko, "Tactile-direction-sensitive and stretchable electronic skins based on human-skin-inspired interlocked microstructures," ACS nano, vol. 8, no. 12, pp. 12 020–12 029, 2014.

[17] G. Cannata, M. Maggiali, G. Metta, and G. Sandini, "An embedded artificial skin for humanoid robots," in 2008 IEEE International conference on multisensor fusion and integration for intelligent systems. IEEE, 2008, pp. 434–438.

[18] T. P. Tomo, M. Regoli, A. Schmitz, L. Natale, H. Kristanto, S. Somlor, L. Jamone, G. Metta, and S. Sugano, "A new silicone structure for uskin—a soft, distributed, digital 3-axis skin sensor and its integration on the humanoid robot icub," IEEE Robotics and Automation Letters, vol. 3, no. 3, pp. 2584–2591, 2018.

[19] A. Maslyczyk, J.-P. Roberge, V. Duchaine et al., "A highly sensitive multimodal capacitive tactile sensor," in 2017 IEEE International Conference on Robotics and Automation (ICRA). IEEE, 2017, pp. 407–412.

[20] S. Youssefi, S. Denei, F. Mastrogiovanni, and G. Cannata, "Skinware: A real-time middleware for acquisition of tactile data from large scale robotic skins," in 2014 IEEE International Conference on Robotics and Automation (ICRA). IEEE, 2014, pp. 6421–6426.

[21] Y. Ohmura, Y. Kuniyoshi, and A. Nagakubo, "Conformable and scalable tactile sensor skin for curved surfaces," in Proceedings 2006 IEEE International Conference on Robotics and Automation, 2006. ICRA 2006. IEEE, 2006, pp. 1348–1353.

[22] M. Fritzsche, N. Elkmann, and E. Schulenburg, "Tactile sensing: A key technology for safe physical human robot interaction," in Proceedings of the 6th International Conference on Human-robot Interaction, 2011, pp. 139–140.

[23] H. Shirado, Y. Nonomura, and T. Maeno, "Realization of human skin-like texture by emulating surface shape pattern and elastic structure," in 2006 14th Symposium on Haptic Interfaces for Virtual Environment and Teleoperator Systems. IEEE, 2006, pp. 295–296.

[24] A. Schmitz, P. Maiolino, M. Maggiali, L. Natale, G. Cannata, and G. Metta, "Methods and technologies for the implementation of large-scale robot tactile sensors," IEEE Transactions on Robotics, vol. 27, no. 3, pp. 389–400, 2011.

[25] T. Minato, Y. Yoshikawa, T. Noda, S. Ikemoto, H. Ishiguro, and M. Asada, "Cb2: A child robot with biomimetic body for cognitive developmental robotics," in 2007 7th IEEE-RAS International Conference on Humanoid Robots. IEEE, 2007, pp. 557–562.

[26] V. J. Lumelsky, M. S. Shur, and S. Wagner, "Sensitive skin," IEEE Sensors Journal, vol. 1, no. 1, pp. 41–51, 2001.

[27] T. Hoshi and H. Shinoda, "Robot skin based on touch-area-sensitive tactile element," in Proceedings 2006 IEEE International Conference on Robotics and Automation, 2006. ICRA 2006. IEEE, 2006, pp. 3463–3468.

[28] M. Teyssier, G. Bailly, C. Pelachaud, E. Lecolinet, A. Conn, and A. Roudaut, "Skin-on interfaces: A bio-driven approach for artificial skin design to cover interactive devices," in Proceedings of the 32nd Annual ACM Symposium on User Interface Software and Technology, 2019, pp. 307–322.

[29] K. Hwang, H. Kim, and D. J. Kim, "Thickness of skin and subcutaneous tissue of the free flap donor sites: a histologic study," Microsurgery, vol. 36, no. 1, pp. 54–58, 2016.

[30] B. P. Pereira, P. W. Lucas, and T. Swee-Hin, "Ranking the fracture toughness of thin mammalian soft tissues using the scissors cutting test," Journal of Biomechanics, vol. 30, no. 1, pp. 91–94, 1997.

[31] A. Laurent, F. Mistretta, D. Bottigioli, K. Dahel, C. Goujon, J. F. Nicolas, A. Hennino, and P. E. Laurent, "Echographic measurement of skin thickness in adults by high frequency ultrasound to assess the appropriate microneedle length for intradermal delivery of vaccines," Vaccine, vol. 25, no. 34, pp. 6423–6430, 2007.

[32] A. Vallbo, R. S. Johansson et al., "Properties of cutaneous mechanoreceptors in the human hand related to touch sensation," Hum Neurobiol, vol. 3, no. 1, pp. 3–14, 1984.

[33] R. S. Johansson and A. Vallbo, "Tactile sensibility in the human hand: relative and absolute densities of four types of mechanoreceptive units in glabrous skin." The Journal of physiology, vol. 286, no. 1, pp. 283–300, 1979.

[34] J. C. Stevens and K. K. Choo, "Spatial acuity of the body surface over the life span," Somatosensory & motor research, vol. 13, no. 2, pp. 153–166, 1996.

[35] T. Schlereth, W. Magerl, and R.-D. Treede, "Spatial discrimination thresholds for pain and touch in human hairy skin," Pain, vol. 92, no. 1-2, pp. 187–194, 2001.

[36] J. Lee, M. T. Cole, J. C. S. Lai, and A. Nathan, "An analysis of electrode patterns in capacitive touch screen panels," Journal of display technology, vol. 10, no. 5, pp. 362–366, 2014.

[37] P. Coni, J. N. Perbet, Y. Sontag, and J. C. Abadie, "31.2: Eliminating ghost touches on a self-capacitive touch-screen," in SID Symposium Digest of Technical Papers, vol. 43, no. 1. Wiley Online Library, 2012, pp. 411–414.

[38] M. Weigel, T. Lu, G. Bailly, A. Oulasvirta, C. Majidi, and J. Steimle, "Iskin: flexible, stretchable and visually customizable on-body touch sensors for mobile computing," in Proceedings of the 33rd Annual ACM Conference on Human Factors in Computing Systems, 2015, pp. 2991–3000.

[39] J. C. Case, M. C. Yuen, J. Jacobs, and R. Kramer-Bottiglio, "Robotic skins that learn to control passive structures," IEEE Robotics and Automation Letters, vol. 4, no. 3, pp. 2485–2492, 2019.

[40] M. Teyssier, G. Bailly, C. Pelachaud, and E. Lecolinet, "Mobilimb: Augmenting mobile devices with a robotic limb," in Proceedings of the 31st Annual ACM Symposium on User Interface Software and Technology, 2018, pp. 53–63.

[41] M. Teyssier, M. Koelle, P. Strohmeier, B. Fruchard, and J. Steimle, "Eyecam: Revealing relations between humans and sensing devices through an anthropomorphic webcam," in Proceedings of the 2021 CHI Conference on Human Factors in Computing Systems. ACM, 2021.

[42] Y. Wang, C. Gregory, and M. A. Minor, "Improving mechanical properties of molded silicone rubber for soft robotics through fabric compositing," Soft robotics, vol. 5, no. 3, pp. 272–290, 2018.
[43] M. Geerligs, "A literature review of the mechanical behavior of the stratum corneum, the living epidermis and the subcutaneous fat tissue," Philips Research, Tech. Rep., 2006.
[44] M.-A. Lacasse, V. Duchaine, and C. Gosselin, "Characterization of the electrical resistance of carbon-black-filled silicone: Application to a flexible and stretchable robot skin," in 2010 IEEE International Conference on Robotics and Automation. IEEE, 2010, pp. 4842–4848.
[45] E. Dean-Leon, J. R. Guadarrama-Olvera, F. Bergner, and G. Cheng, "Whole-body active compliance control for humanoid robots with robot skin," in 2019 International Conference on Robotics and Automation (ICRA). IEEE, 2019, pp. 5404–5410.
[46] A. Cirillo, F. Ficuciello, C. Natale, S. Pirozzi, and L. Villani, "A conformable force/tactile skin for physical human–robot interaction," IEEE Robotics and Automation Letters, vol. 1, no. 1, pp. 41–48, 2015.
[47] M. M. Jung, R. Poppe, M. Poel, and D. K. Heylen, "Touching the void–introducing cost: corpus of social touch," in Proceedings of the 16th International Conference on Multimodal Interaction, 2014, pp. 120–127.
[48] M. Sigalas, H. Baltzakis, and P. Trahanias, "Gesture recognition based on arm tracking for human-robot interaction," in 2010 IEEE/RSJ International Conference on Intelligent Robots and Systems. IEEE, 2010, pp. 5424–5429.
[49] H. K. Graham, J. C. McConnell, G. Limbert, and M. J. Sherratt, "How stiff is skin?" Experimental Dermatology, vol. 28, pp. 4–9, 2019.
[50] B. Davison, "Techniques for robust touch sensing design," AN1334 Microchip Technology Inc, vol. 53, 2010.
[51] T. P. Tomo, A. Schmitz, W. K. Wong, H. Kristanto, S. Somlor, J. Hwang, L. Jamone, and S. Sugano, "Covering a robot fingertip with uskin: A soft electronic skin with distributed 3-axis force sensitive elements for robot hands," IEEE Robotics and Automation Letters, vol. 3, no. 1, pp. 124–131, 2017.
[52] Y.-L. Park, B.-R. Chen, and R. J. Wood, "Design and fabrication of soft artificial skin using embedded microchannels and liquid conductors," IEEE Sensors journal, vol. 12, no. 8, pp. 2711–2718, 2012.
[53] S. Yohanan and K. E. MacLean, "The role of affective touch in human-robot interaction: Human intent and expectations in touching the haptic creature," International Journal of Social Robotics, vol. 4, no. 2, pp. 163–180, 2012.
[54] M. J. Hertenstein, D. Keltner, B. App, B. A. Bulleit, and A. R. Jaskolka, "Touch communicates distinct emotions." Emotion, vol. 6, no. 3, p. 528, 2006.
[55] D. Hughes, J. Lammie, and N. Correll, "A robotic skin for collision avoidance and affective touch recognition," IEEE Robotics and Automation Letters, vol. 3, no. 3, pp. 1386–1393, 2018.